Sensors and Actuators B: Chemical. Vol. 67, Issue 3, 1 September 2000, Pages 227-234

# Comparison of self-referencing techniques for photothermal detection of trace compounds in water

Jane Hodgkinson[#*H], Mark Johnson[#] and John P. Dakin*

[#] North West Water Ltd, Dawson House, Great Sankey, Warrington WA5 3LW
* Optoelectronics Research Centre, Mountbatten Building, University of Southampton, Highfield, Southampton SO17 1BJ
[H] Now at: BG Technology, Gas R&T Centre, Ashby Rd, Loughborough, Leics LE11 3GR

## Abstract

Self-referencing techniques are compared for a closed-cell photothermal detector that uses a water meniscus as a pressure sensor. Deflection of the meniscus was measured using an optical fibre Fabry-Perot interferometer. For long measurement integration times, interference fringe drift was a serious limitation on the detection repeatability for non self-referenced measurements. Two self-referencing techniques were compared for measurements of optical absorption. The first used a simultaneous reference absorption signal at a second wavelength, and the second used a simultaneous volumetric modulation within the cell. Both methods have been evaluated with photothermal excitation by a 658nm LED, a 478nm LED and a UV discharge lamp. For the detection of absorption in aqueous solutions, the two methods had similar performance. However, the volumetric method could be used for detection of any absorbing compound, regardless of its absorption spectrum, and was more convenient to use.

## 1 Introduction

A closed-cell, low-frequency photothermal detector that uses a water meniscus as a sensor has been shown to offer highly sensitive detection of trace compounds in aqueous solution[1]. This is particularly important if low power light sources are to be used, such as laser diodes, LEDs and UV discharge lamps. In general, photothermal signals are directly proportional to the incident light intensity[2,3]. If the signal to noise ratio of the detector is to be maintained when using low incident powers, close attention must be paid to the limiting sources of noise in the system, because the signal is so small.

The water meniscus in our detector is constrained by surface forces at the top of the closed cell, where it acts as a pressure sensor. Vertical movement of the centre of the meniscus is detected using fibre optic interferometry. This approach enhances the sensitivity of the system, but has suffered from the disadvantage that the fringe depth must be measured, and phase quadrature maintained, in order for the interference fringes to be demodulated. Over long measurement integration times, it has been found that the interference fringes may drift, resulting in a scale change in the final signal. The effect reduces the repeatability of the technique, and thus has acted as an important limitation when the species to be detected absorbed less than its solvent, water. In particular, when detecting UV-absorbing compounds such as anthracene, the relatively high absorption coefficient of water at 254nm necessitates further discrimination of the relatively small additional signal due to the analyte.

Two self-referencing methods have been used to improve the repeatability of the photothermal system. The first used a second excitation beam at a longer wavelength, which was not absorbed by the analyte and could be modulated at a different frequency from the main (254 nm) excitation beam. The resulting photothermal reference signal, expected to be due to the water background alone, was used to scale the 254nm results. This method has been previously reported in an earlier paper[4], but the results are also presented here for comparison purposes. In this paper, we report a further development of the photothermal technique, in which a volumetric reference signal is generated simultaneously with the photothermal signal. This second self-referencing method has the advantage of being generally applicable to any absorbing compound, regardless of its absorption spectrum. Results are presented for detection of potassium permanganate ($KMnO_4$) at 254nm and other excitation wavelengths.

## 2 Principle of operation

A schematic diagram of the cell is shown in Figure 1. It employs a flat water meniscus, constrained by surface forces, at a small circular pinhole in nickel foil. Photothermal absorption of modulated light resulted in periodic pressure changes in the cell, which caused the meniscus to be deflected like a thin diaphragm, its curvature determined by the excess pressure in the cell. Zero dc pressure difference across the meniscus was maintained by a slow hydraulic leak to an outside reservoir, which equalised internal and external pressures on a timescale much longer than the photothermal modulation period. This arrangement kept the meniscus approximately flat, with small deflections from the mean position.

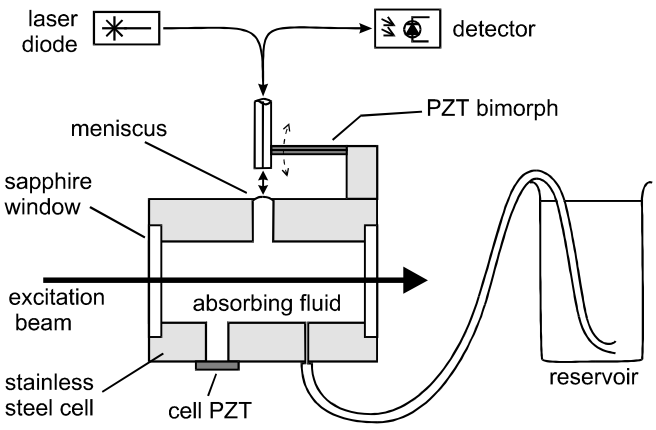


Figure 1. Schematic diagram of the photothermal cell.

Vertical movement of the centre of the meniscus was detected using fibre optic interferometry. The centre of the meniscus and the cleaved end of a single-mode optical fibre formed a low finesse interference cavity, with a distance of approximately 60μm maintained between the two, to prevent accidental contact. While this reduced the coupling efficiency of the reflected light into the fibre, the sensitivity of the photothermal measurements was not found to be affected.

## 3 Theory of operation

The absorbed intensity $I$ of a sample with an absorption coefficient $\alpha$ (in $cm^{-1}$) and optical pathlength $L$ (in cm) is given by Beer's law. The absorbed light intensity is;

$$I = I_0 \left(1 - 10^{-\alpha L}\right) \tag{1}$$

where $I_o$ is the incident intensity. Following this energy absorption, the deflection of the centre of the meniscus, $\Delta h$, has been shown[1] to be equal to the following;

$$\frac{\partial \Delta h}{\partial E} = \frac{\beta a^2}{4 C_p \rho \gamma} \frac{1}{\left(\frac{V_c}{\kappa} + \frac{\pi a^4}{8\gamma}\right)} \tag{2}$$

$E$ is the light energy absorbed by the fluid, $\beta$ is the volume thermal expansion coefficient of the fluid, $C_p$ is its specific heat capacity, $\rho$ is its density, $\gamma$ is its surface tension, $\kappa$ is its bulk modulus, $a$ is the radius of the meniscus (200μm), and $V_c$ is the volume of fluid enclosed by the cell ($1.6\times10^{-5}$ $m^3$). We assume that all the light absorbed by the solution is instantly converted to heat.

Detection of meniscus deflection, $\Delta h$, is by fibre optic interferometry. The cleaved fibre end of the interferometer and the centre of the water meniscus form a low finesse Fabry-Perot cavity, whose interference fringes are given by,

$$\mathrm{v} = \mathrm{v}_0 + A \cos\left(\frac{4\pi d}{\lambda}\right) \tag{3}$$

where v is the voltage signal from the detector (proportional to the detected fringe intensity), $d$ is the distance separating the fibre end and the meniscus, $\lambda$ is the interferometer wavelength, and $A$ is a scale factor which is to be determined. At phase quadrature, the meniscus deflection may be calculated from the detected voltage signals using the equation;

$$\delta \mathrm{d} = \delta \mathrm{v} \cdot \frac{\lambda}{4\pi A} \tag{4}$$

The responses of all the elements of the system may be brought together and expressed as follows. The photothermal response is measured as a voltage signal v from the interferometer detector according to the following equation:

$$\begin{aligned} \mathrm{v}_{\mathrm{rms}} &= \frac{\partial \mathrm{v}}{\partial \mathrm{h}} \frac{\partial \Delta \mathrm{h}}{\partial E} \Delta E_{\mathrm{rms}} \\ &= \frac{\lambda}{4\pi A} \frac{a^2}{4\gamma\left(\frac{\mathrm{V_c}}{\kappa} + \frac{\pi a^4}{8\gamma}\right)} \frac{\beta}{\mathrm{C_p}\,\rho} \frac{I_{\mathrm{rms}}}{f}\left(1 - 10^{-\alpha \ell}\right) \end{aligned} \tag{5}$$

This can be written in terms of a number of possible scale factors, given as functions of those variables most likely to change during or between measurements:

$$\mathrm{v}_{\mathrm{rms}} = F(A)\; R(\gamma)\; P(T) \frac{I_{\mathrm{rms}}}{f}\left(1 - 10^{-\alpha \ell}\right) \tag{6}$$

$F$ is an interference fringe scale factor, $R$ is a cell responsivity scale factor (dependent on the mechanical compliance of the cell and the surface tension of the fluid) and $P$ is a photothermal volume expansion factor, which is a strong function of temperature. Equation (6) can also be written as a function of a periodic volume change within the cell:

$$v_{rms} = F(A)\ R(\gamma)\ \Delta V \quad (7)$$

where $\Delta V$ is the volume change of the fluid, which might be photothermal in origin or be directly initiated in the cell. Errors or uncertainty in any of the above scale factors would lead to measurement repeatability errors. In the photothermal self-reference technique, a standard periodic photothermal signal (constant $P$ in equation (6)) was applied, giving a reference signal v. In the volumetric technique, a standard periodic volumetric signal (constant $\Delta V$ in equation (7)) was applied to give a second type of reference signal v. Thus, the both types of reference could potentially correct for changes in the interference fringe height ($A$), the surface tension of the fluid ($\gamma$) and changes in the mechanical compliance of the cell (also affecting $R$). In addition, the photothermal reference could also potentially correct for changes in temperature ($T$).

## 4 Experimental

The system has been described in greater detail[1], but the essential characteristics are presented here. The stainless steel cell had a cylindrical internal bore of length 50mm and radius 10mm. The water meniscus was formed at a 200μm radius pinhole in nickel foil. A schematic diagram of the detection system is shown in Figure 2.

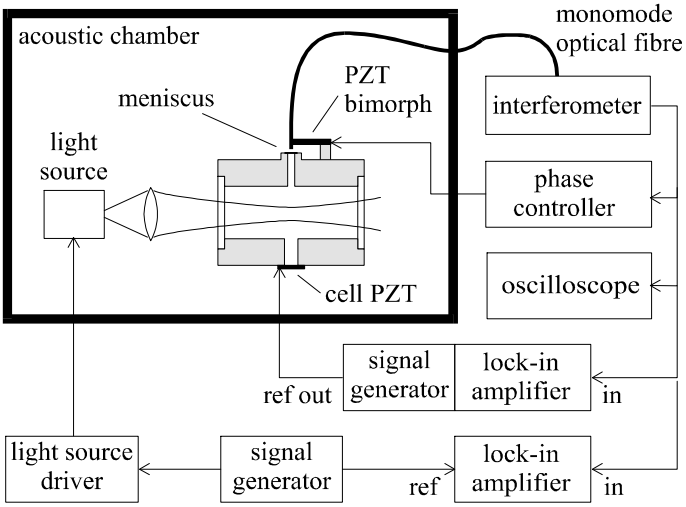


Figure 2. Schematic diagram of the system used for photothermal detection.

The full interferometer system is shown in Figure 3. Phase quadrature was maintained in the interferometer using a piezoelectric bimorph element (Quantelec EB-T-320), which moved the cleaved fibre end in relation to the meniscus. A feedback control circuit maintained a predetermined dc output from the interferometer receiver by applying a variable voltage to the bimorph, thus mechanically tracking an interference fringe edge. The photodiode at (2) was connected to a transimpedance amplifier, giving a voltage signal v, which was converted to a displacement d using equation (4). The interferometer was used to measure the relative meniscus displacement with an rms noise floor of 10 pm $Hz^{-1/2}$.

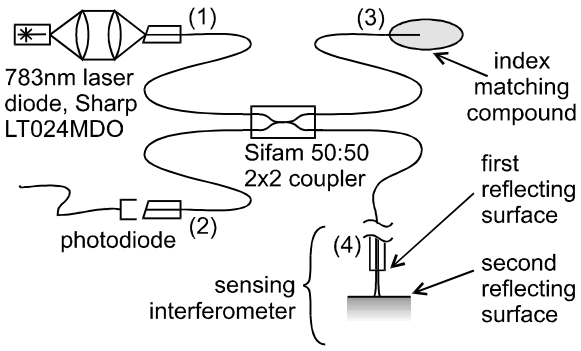


Figure 3. Low finesse fibre Fabry-Perot interferometer, used to detect the relative position of the meniscus

Three types of light sources were used for our experiments. The first was a red laser diode module (RS 194-004) which could be square-wave modulated with an output power of 1.4 mW rms at 678nm. The second were two visible LEDs: a blue LED (Marl 110106) emitting 0.75±0.11 mW at a peak of 478 nm, and a red LED (LED Technology LURR3000G3) emitting 0.88±0.13 mW at a peak of 658 nm. Each was driven at 70Hz using a square-wave voltage from a signal generator (Thurlby Thandar TG220) with a 220Ω resistor in series to give a peak drive current of 30mA. The final light source was a mercury discharge lamp (Spectronics Spectroline 11SC-1), driven via its proprietary driver (Spectroline SCT 1A/F), which was designed to run from a mains input. Variable frequency operation was achieved by connecting the signal generator output to a power amplifier (ILP SMOS 248), and using a transformer (RS 578-430) to provide the 240V required by the lamp driver. The lamp intensity was modulated as a rectified sin wave, the majority of the modulation occurring at 2f. The 2f-modulated output power was found to be 0.3 ±0.05 mW rms at 254nm. Stray light was reduced by covering the mercury tube with aluminium foil, apart from a 3mm hole from which light was coupled into the cell using a high NA lens.

Photothermal signals detected with an EG+G 5210 phase sensitive lock-in amplifier in “f” mode, or “2f” mode if the UV lamp was being used. A second lock-in amplifier was employed to detect reference signals (EG+G 5110), differing from the first only in its upper frequency limit. Both lock-ins employed 100s integration periods. The cell PZT (Morgan Matroc PZT-5A) was a 0.45mm thick, 10mm square wafer, with electrodes on the two opposing faces, bonded to a 6mm diameter hole in the cell wall.

Experiments were performed on aqueous solutions of anthracene and potassium permanganate ($KMnO_4$). $KMnO_4$ is known to be a good standard for use as a photoacoustic absorber[5], enabling our results to be translated to other compounds. The absorption of $KMnO_4$ in each test solution was determined with a diode array spectrometer (HP 8452A). Measured absorption spectra of anthracene and $KMnO_4$ are shown in Figure 4 and Figure 5.

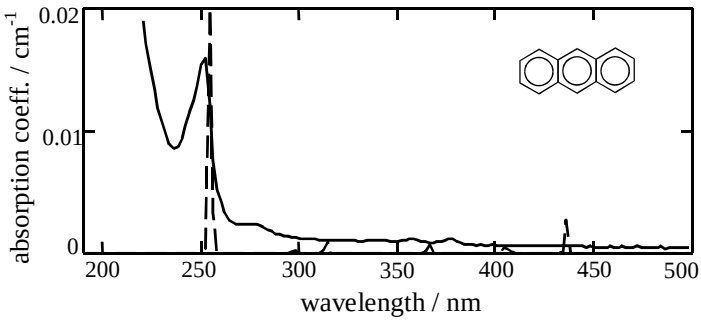


Figure 4. Absorption of 14ppb anthracene in aqueous solution (solid line), taken against a deionised water blank. The emission spectrum of the mercury lamp (dashed line, arbitrary units) has been superimposed.

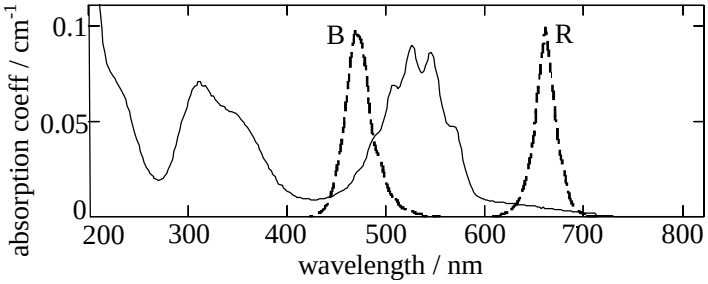


Figure 5. Absorption spectrum of 5ppm $KMnO_4$ in solution (solid line), with the normalised emission spectra of the blue and red LEDs superimposed (dashed lines).

The experimental procedure was as follows. The cell was rinsed with the solution to be tested, and then filled so as not to incorporate air bubbles. The interferometer fibre was roughly aligned to the centre of the meniscus, by eye, using an xyz stage. A sinusoidal voltage of approximately 10V peak-to-peak was applied to the cell PZT in order to modulate the height of the centre of the meniscus. The resulting fringes from the interferometer were displayed on an oscilloscope and used to align the fibre more precisely, to the position of maximum meniscus movement. Photothermal measurements were made with or without a self-reference signal, as described in more detail in each of the following sections.

## 5 Results

### 5.1 Photothermal detection without a self-reference

Before measurements using this method began, a large (approximately 10Vp-p) signal was applied to the cell PZT, at the same frequency as the intended photothermal modulation. The resulting full height interference fringes were used to determine both the value of *A* in equation (3) and the phase quadrature setpoint. The magnitude of the response to the cell PZT signal was also used to normalise the cell sensitivity. Further scaling was performed to correct for the temperature dependence of $\beta$ in equation (5). It was assumed that the test solutions were at the laboratory temperature, which varied between 20°C and 25°C. The data were then normalised to a temperature of 20°C. Thus, to first order, scale factors F, R and P in equation (6) could be approximately determined.

The UV discharge lamp was used to excite photothermal signals in solutions of anthracene in deionised water. The resulting measured meniscus deflections are shown in Figure 6 versus anthracene concentration in ppb by weight. The blue and red LEDs were used to excite similar signals in various concentrations of $KMnO_4$, also in deionised water. In this case, results have been plotted against the absorption coefficients of the solutions, to enable our results to be extrapolated to other compounds. At low concentrations, the signals reached a plateau corresponding to the background level of water absorption; the mean measured photothermal signal for deionised water is shown as a dashed line.

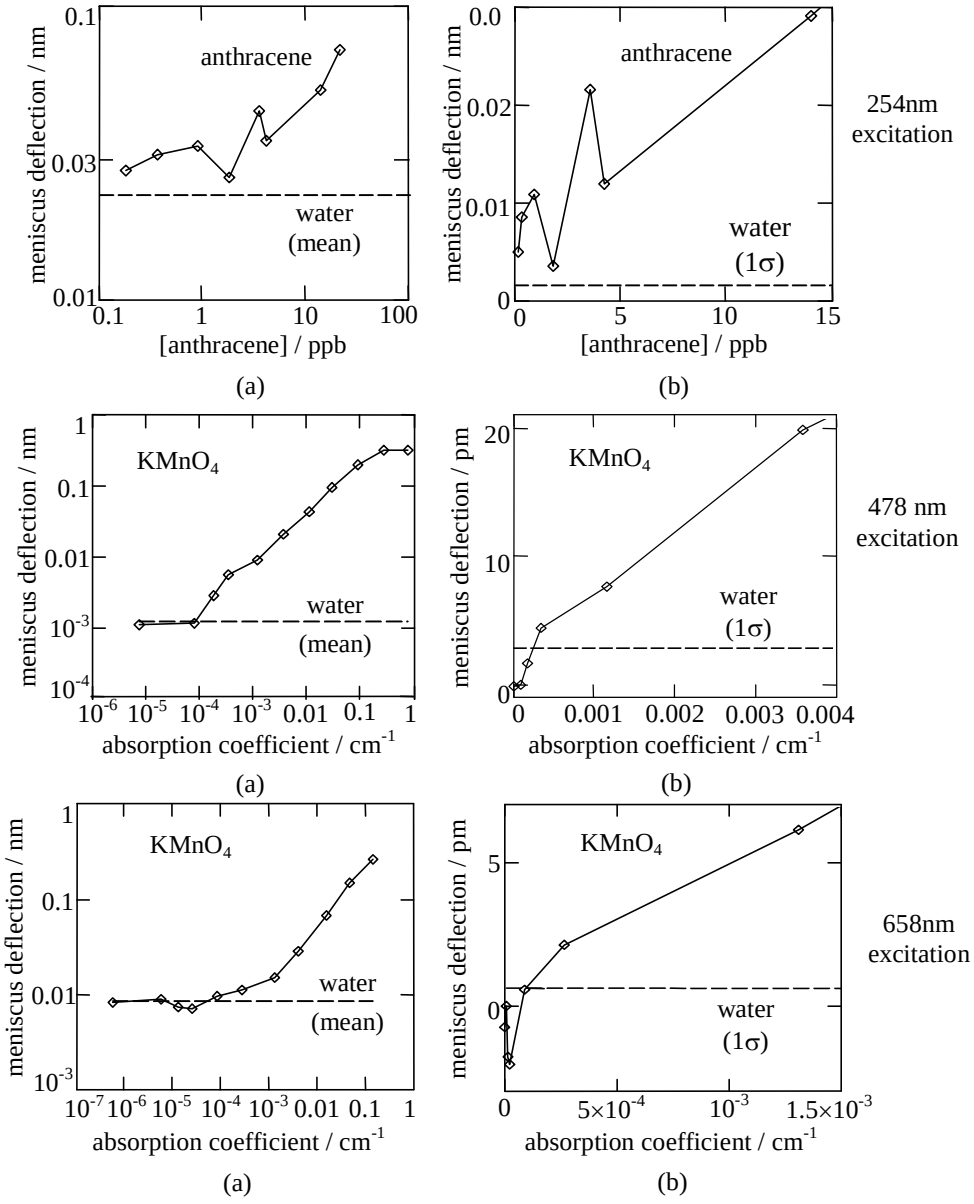


Figure 6. Photothermal rms meniscus deflection excited in $KMnO_4$ solutions by a 478nm and 658nm LED (as previously published [4].) and in anthracene solutions by a mercury discharge lamp. (a) Original data. (b) The same data following subtraction of the mean measurement for water.

Further discrimination of the small additional absorption of the target compound was be obtained by arithmetically subtracting the photothermal signal measured using a deionised water blank. This gave a linear dependence on concentration at low concentrations above the noise level. At 478nm, the background absorption of water is relatively low ($1.1\times10^{-4}$ $cm^{-1}$,[6]), but at 658nm and 254 nm it is higher ($1.4\times10^{-3}$ $cm^{-1}$ [6] and $7\times10^{-3}$ $cm^{-1}$ [7], respectively). At these wavelengths, the measurement repeatability limited the minimum detectable concentration, and can be defined as the value of one standard deviation ($1\sigma$) for a number of measured signals from blank deionised water samples, as also shown in Figure 6 (b). For anthracene at 254nm, the limit of detection was approximately 5-10 ppb, which was significantly worse than expected. For a measurement integration period of 100s, the meniscus deflection noise of 10 pm $Hz^{-1/2}$ should give a minimum detectable meniscus deflection of 1 pm, rather than the 10 pm limit that was experimentally demonstrated.

The repeatability of the photothermal measurements was believed to be limited by the interferometric phase demodulation technique, for which it was assumed that the interference fringes remained stable over the entire measurement integration period (100s). However, it was observed that the interference fringe depth ($A$) could drift by as much as 30% over a measurement period. The fringe depth and quadrature point were checked at the end of each measurement, and if found to have changed by more than approximately 10%, the measurement was repeated. However, there was no means of checking the fringe stability during each measurement.

### 5.2 Dual wavelength, self-referenced photothermal measurements

Anthracene's absorption spectrum made it an ideal candidate for this self-referencing method. At 254nm, its absorption coefficient is relatively high, but at much longer wavelengths its absorption is negligible compared to the background absorption of water. A second signal at 678nm should provide a reliable reference, whose magnitude is independent of the concentration of the target compound and merely depends on the absorption of water at that wavelength.

For dual wavelength self-referenced measurements, the experimental configuration was identical to that shown in Figure 2, with one important difference. Emission from two light sources (the mercury discharge lamp and the 678nm laser diode described previously) was simultaneously directed into the cell, each from opposite ends. The UV lamp was driven at a frequency of $2f$ = 115Hz as before, and the signal detected using the same lock-in amplifier in R, $\theta$ mode with a 100s time constant. A second signal generator of the same type as the first was used to drive the laser diode at a frequency of 70Hz. The 70Hz photothermal signal was detected using a second lock-in amplifier (EG&G 5110), which differed from the first only in its upper frequency limit (100kHz rather than 120kHz).

The photothermal response consisted of superimposed signals at the two different modulation frequencies. It was important for the 678nm-excited reference signal and the 254nm-excited measurement signal to be detected simultaneously, using equipment with the same filtering characteristics. Therefore, the second lock-in amplifier was used in the same operational mode as the first. Cross-talk between the photothermal signals excited at the two different frequencies was established to be at or below the measurement noise level.

At 678nm, anthracene was expected to exhibit negligible absorption at each of the concentrations tested. The water was expected to show a relatively significant and measurable level of absorption at both the excitation wavelengths. The measured photothermal signals ($S$) for low levels of absorption at 678nm and 254nm are then given by the following:

$$S_{254} = P\left[\alpha_{w,254} + \alpha_{a,254}\right]\frac{I_{254}}{f_1}$$
$$S_{678} = P\,\alpha_{w,678}\,\frac{I_{678}}{f_2} \tag{8}$$

where $I_{254}$ and $I_{678}$ are the emitted powers of the UV lamp and the laser diode, and P is a scale factor to be determined, which depends on (a) the cell responsivity, and (b) the interference fringe height. The subscripts "w" and "a" denote water and anthracene, respectively. Taking blank reference measurements (*R*) with deionised water gives a second pair of equations, with a second scale factor Q.

$$R_{254} = Q\,I_{254}\,\alpha_{w,254}\,\frac{I_{254}}{f_1}$$
$$R_{678} = Q\,I_{678}\,\alpha_{w,678}\,\frac{I_{678}}{f_2} \tag{9}$$

We assume that the following parameters remain constant: the level of absorption of the water at 678nm (expected to be $1.8\times10^{-3}$ $cm^{-1}$ [6]), the emitted powers of the excitation sources and the modulation frequencies. Forming ratios of the 254nm signals to the 678nm signals, and subtracting the blank reference, then gives a measurement of the quantity of anthracene in solution.

$$\frac{S_{254}}{S_{678}} - \frac{R_{254}}{R_{678}} = \frac{\alpha_{a,254}}{\alpha_{w,678}}\,\frac{I_{254}}{I_{678}}\,\frac{f_2}{f_1} \tag{10}$$

The ratio of the 254nm-excited photothermal meniscus deflection signal to the 678nm-excited signal, for each sample, has been plotted in Figure 7 (a) against the estimated anthracene concentration in ppb by weight. Also shown is the mean of the photothermal signal ratios measured using deionised water (dashed line). The same data are shown in Figure 7 (b), following subtraction of the mean measured ratio for water. The dashed line shows the level of one standard deviation in the measured signals for water.

These results indicate that our technique may be used to detect anthracene in aqueous solution at levels down to approximately 2ppb or below (SNR=1), corresponding to an absorption coefficient of $1.7\times10^{-3}$ $cm^{-1}$. This is consistent with the measurement being limited by a minimum detectable meniscus deflection of the order of 1pm, and is a significant improvement over the results obtained with no self-referencing, shown in Figure 6.

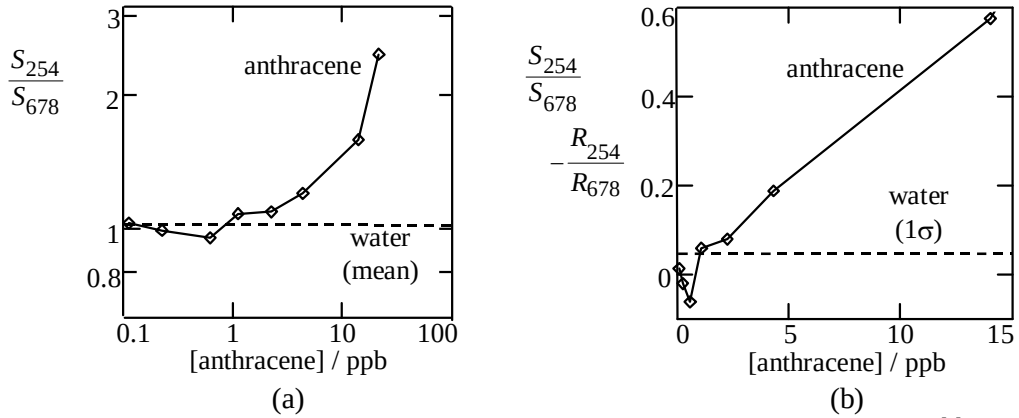


Figure 7. Photothermal results for anthracene and deionised water, as previously published[1]. (a) Ratio of 254nm-excited to 678nm-excited signals. (b) The same data following subtraction of the mean ratio for water.

### 5.3 Self-referencing using volume changes applied by the cell PZT

This self-referencing technique was tested using $KMnO_4$, whose complex absorption spectrum rendered it unsuitable for the dual wavelength method. A low-frequency volumetric reference signal was provided by the cell PZT (see Figure 1), driven by a sinusoidal voltage from a signal generator. The resulting volume displacement was proportional to the magnitude of the drive signal. This modulation was small yet consistent, causing a small sinusoidal meniscus deflection that could be detected simultaneously with the photothermal signals generated within the fluid (each at a different frequency). Phase sensitive detection of the photothermal signal and the PZT-applied signal proceeded simultaneously, using two lock-in amplifiers, the modulation frequencies chosen for maximum signal / noise ratio and minimum mutual cross-talk.

The signal applied to the cell PZT, for self-referencing purposes, was 9.48 mV rms at 90 Hz. Photothermal signals were generated at 115Hz, as before. Cross-talk between the two simultaneous signals was confirmed to be negligible. The phase quadrature setpoint for the fibre optic interferometer was determined in the same way as before, but only an approximate setting was needed in this case.

#### 5.3.1 Self reference calibration

It was desirable to find the correlation between (a) the signals resulting from a voltage applied to the cell PZT, and (b) the scale factors that would otherwise have been measured, namely fringe depth and cell sensitivity. The latter enabled the photothermal signals, in volts, to be converted to meniscus deflection, in nm. A number of photothermal experiments were performed for a variety of different interference fringe depths and laboratory temperatures, measured over the usual 100s integration period. The scale factors used in section 5.2 were measured before and after each measurement, as well as the reference voltage signal resulting from the simultaneous modulation of the cell PZT during the experiment. The cell PZT was found to displace the centre of the meniscus centre by 82±7 nm per volt applied across the PZT electrodes. For an applied voltage of 9.48mVrms, the photoacoustic meniscus deflection may be calculated from the measured photoacoustic signals and the simultaneously measured cell PZT signals, as follows.

$$\Delta h \quad = \quad (0.78 \pm 0.07)\text{nm} \cdot \frac{\text{PA signal}}{\text{PZT signal}} \tag{11}$$

It is useful to know the rms levels of meniscus deflection in our experiments, to compare them to the measured displacement noise of 10 pm $Hz^{-1/2}$.

Figure 8 shows the correlation obtained between (a) the measured signal resulting from a cell PZT-applied voltage 0f 9.48mVrms, and (b) the level of that signal predicted using equation (11) and the measured interference fringe depth. We expect the two measurements to be equivalent, the best fit line having unit gradient and passing through the origin. The scatter of data points about the best-fit line can be entirely accounted for by possible fringe drift, which could give an error in the calculated meniscus deflection of up to 30%, but more typically of the order of 10%, depending on the conditions.

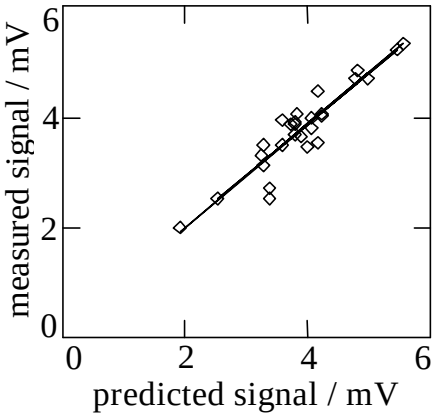


Figure 8. Correlation between the reference signal resulting from the cell PZT modulation, and the signal level predicted using equation (11), showing that they are equivalent.

### 5.3.2 Results using volumetric self-referencing

Simultaneous photothermal and volumetric reference signals were recorded and used to derive the photothermal meniscus deflection using equation (11). These results are shown in Figure 9, plotted as a function of the absorption coefficient of $KMnO_4$.

For UV absorption, this self-referencing technique appears to give a minimum detectable absorption coefficient that is similar to the dual-wavelength method. At 478nm and 658nm, there is little if any performance improvement compared to results which had no self-referencing. However, the data taken at 658nm appear to show less scatter than the uncompensated data presented in Figure 6. The LED-excited data for self-referenced and uncompensated experiments were taken at the same time. Any variability, due for example to temperature fluctuations or interference fringe drift, should have affected both techniques, enabling a direct comparison to be made.

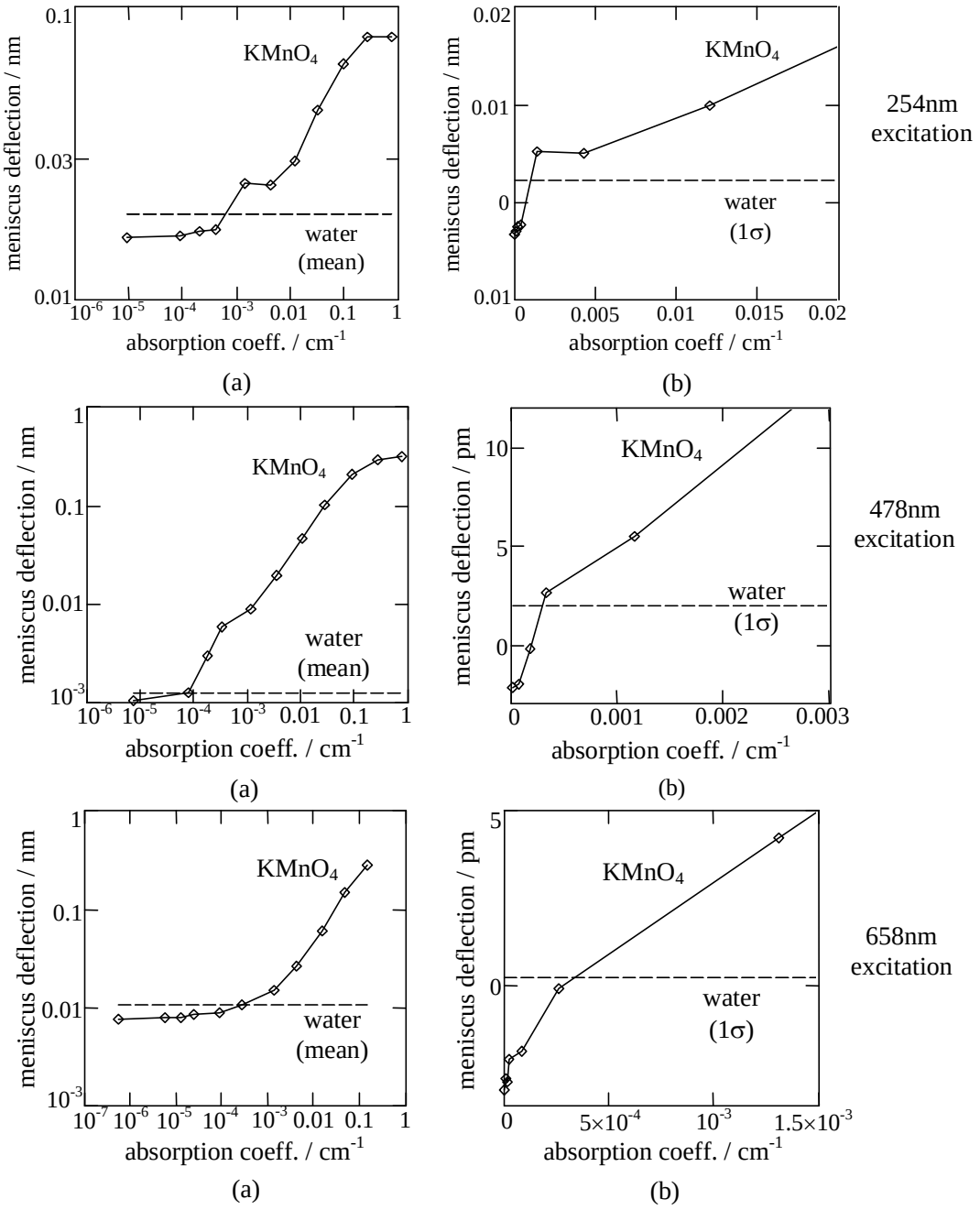


Figure 9. Photothermal meniscus deflection signals obtained using volumetric self-referencing for $KMnO_4$ solutions at 254nm, 478nm and 658nm. (a) Raw data. (b) The same data following subtraction of the mean result for a DI water control.

## 6 Discussion of self-referencing techniques

We can compare our results using the scale factor analysis of equations (6) and (7). In the absence of self-referencing, scale factors F and R in equation (6) were determined by using the cell PZT to excite large meniscus displacements, and measuring the full height interference fringes thus produced. However, this could only be accomplished before or after the photothermal measurement, during which it was possible for the interference fringes to drift, and the calculated meniscus displacement to be in error. Fringe drift has resulted in errors in the calculated meniscus deflection, estimated to be between 10% and 30% for long measurement integration periods. It was also possible to measure the ambient temperature during the experiment, to compensate for changes in the heat capacity, density and the thermal expansion coefficient of the fluid. The latter, for water, has a strong dependence on temperature. However, this method of temperature compensation is indirect and therefore unsatisfactory.

Dual-wavelength self-referencing offers a scale factor reference signal that is excited and measured photothermally. According to equation (6), it therefore provides full compensation for any possible changes in temperature, mechanical compliance of the cell, solvent properties (such as surface tension) and/or interference fringe drift, which might affect the photothermal response. However, its use is restricted to the detection of compounds, such as anthracene, in which absorption at the reference wavelength is negligible. The reference signal is used to scale the measurement, and any absorption by the analyte at the reference wavelength would simply scale the reference in proportion to the signal, with no benefit.

Volumetric self-referencing relies on a standard (periodic) volume displacement initiated directly in the cell. According to equation (7), it could therefore correct for changes in the surface tension of the fluid, the mechanical compliance of the cell and interference fringe drift. Because the signal was not generated photothermally, a disadvantage would be that this method could not correct for changes in the temperature of the fluid, which would affect the thermal expansion coefficient, $\beta$. However, it could be used to detect analytes with any absorption spectrum, and could therefore be used to detect $KMnO_4$ in water with a high degree of repeatability.

Both methods of self-referencing have improved the measurement repeatability of the photothermal detector. However, neither method can entirely compensate for scaling errors introduced by the interferometer. In both methods, the reference signal is generated at a different frequency to the photothermal signal. It is always possible that the effect of noise or of a transient fringe drift could be different at each of the two frequencies. Nevertheless, we have found experimentally that fringe drift, the main factor responsible for repeatability errors, tends to occur at much lower frequencies and hence should affect measurements at both the signal and reference frequencies in substantially the same way. Both techniques were therefore able to provide improved performance compared to the case where no reference was used.

## 7 Conclusion

In our photothermal detector, a water meniscus is used as a pressure sensor, whose periodic deflection is measured using an optical fibre Fabry-Perot interferometer. Interference fringe drift has been found to limit the repeatability of measurements over long integration periods. This becomes significant when detecting absorption changes at or below the level of the background absorption due to water, and small additional absorption coefficients are discerned by subtraction of a blank reference signal from a control sample.

Two different self-referencing methods have been presented, which have improved the repeatability of

photothermal measurements. In both techniques, a second signal was generated at a different modulation frequency from the photothermal signal, and detected simultaneously. The first technique employed a second reference wavelength to give a photothermal reference, correcting for any variations in the overall responsivity of the system. However, its use relied on the availability of a light source emitting a wavelength that was not absorbed by the analyte. The second self-referencing technique made use of a standard volumetric modulation in the photothermal cell, applied using a piezoelectric transducer. This new method had the advantage of greater convenience and could be used with any analyte, regardless of its absorption spectrum.

**Acknowledgements**

The work was supported by North West Water Ltd and by the EPSRC / Department of Trade and Industry in the UK, through the Teaching Company Scheme.

**References**

1 J. Hodgkinson, M. Johnson and J. P. Dakin, Photothermal detection of trace optical absorption in water by use of visible light emitting diodes, *Applied Optics, 37* (1998) 7320-7326.

2 A. Rosencwaig, *Photoacoustics and photoacoustic spectroscopy,* Wiley, New York, 1980.

3, Y.-H. Pao, *Optoacoustic spectroscopy and detection,* Academic Press, New York, 1977.

4 J. Hodgkinson, M. Johnson and J. P. Dakin, Photoacoustic detection using the deflection of a water meniscus, *Measurement Science and Technology, 9* (1998) 1316-1323.

5. S. E. Braslavsky and G. E. Heibel, Time-resolved photothermal and photoacoustic methods applied to photoinduced processes in solution, *Chemical Review, 92* (1992) 1381-1410.

6. C. K. N. Patel and A. C. Tam, Pulsed optoacoustic spectroscopy of condensed matter, *Reviews of Modern Physics, 53* (1981) 517-550.

7 G. M. Hale and M. R. Querry, Optical constants of water in the 200-nm to 200-μ wavelength region, *Applied Optics, 12* (1973) 555-563.